LAUR-96-3012

SOURCE MOMENT TENSOR ESTIMATION OF SURFACE MINING BLASTS

Xiaoning Yang and Dr. Brian W. Stump

SOURCE MOMENT TENSOR ESTIMATION
OF SURFACE MINING BLASTS

Xiaoning Yang

Department of Geological Sciences
Southern Methodist University
Dallas, TX 75275
Phone: (214) 768-1659
e-mail: yang@passion.isem.smu.edu

Dr. Brian W. Stump

Geophysics Group EES - 3
Los Alamos National Laboratory
Los Alamos, NM 87545
Phone: (505) 667-1004
e-mail: stump@lanl.gov

I. INTRODUCTION

Successful monitoring of the CTBT (Comprehensive Test Ban Treaty) requires the ability to discriminate small scale, possibly decoupled nuclear tests from large surface mining and quarry blasts. This necessity arises from the concern that the magnitude of a small scale, decoupled nuclear explosion is comparable to that of a large surface mining blast and its seismic signal could be hidden by the signal from a mining blast.

Large scale surface mining blasts employ the millisecond delayed blasting technique in which individual shots in an array are detonated in a millisecond-delayed sequence. Investigations into the seismic characteristics and thus discriminants of these so-called "ripple fired" blasts indicate a need for detailed knowledge of the characteristics of the individual single mining shot in the shot array which comprises the blast.

This paper reports the results of a study which characterizes the single mining shot in terms of its source moment tensor representation. The study uses near-source, broad band ground motion data collected in a controlled field experiment composed of 8 single-hole surface mining shot sources. The results reveal characteristics of this particular kind of seismic source which are useful for us to understand the physical source processes involved and improve our discrimination ability

1.716 sec

The field experiment was conducted in a coal mine on a overburden shale bench roughly 150 meters wide and 11 meters high. Fig. 1 sketches the layout of the experiment. All 8 explosion sources, denoted as red dots in the figure, were located 6 meters from the vertical free face of the bench. A 3-component accelerometer array (blue triangles) was deployed on the bench behind the sources covering a range from 48 m to 157 m and an azimuthal spread of 168°.

The sizes of the cylindrical sources range from 59 to 296 kg. Some key source parameters are listed in Table 1. A vertical cross section of the source region is given in Fig. 2 to illustrate the source geometry and the closeness of the sources to the vertical free face and the earth's free surface. In the experiment, the sources were detonated separately. During each shot, the burden was cast into the pit and a crater was formed.

Before the experiment, a refraction survey with both *P* and *S* wave sources was conducted on the test site. Some of the refraction sections are presented in Fig. 3. The resultant test site velocity model is drawn in Fig. 4.

Ground acceleration data from these explosion sources were recovered by the accelerometer array. An example of the ground velocity data integrated from the ground acceleration is given in Fig. 5.
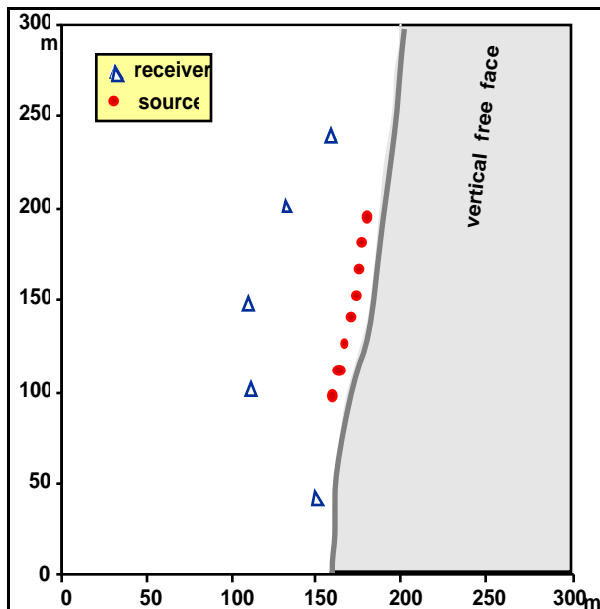

Figure 1 The layout of the experiment. The red dots are mining explosion sources. They are emplaced alon vertical free face of the test bench. The gray area is t of the mine about 11 meters below the bench. The triangles are the accelerometers.
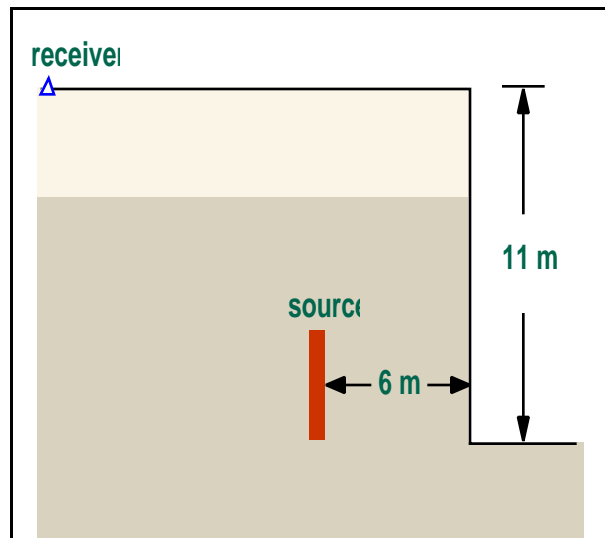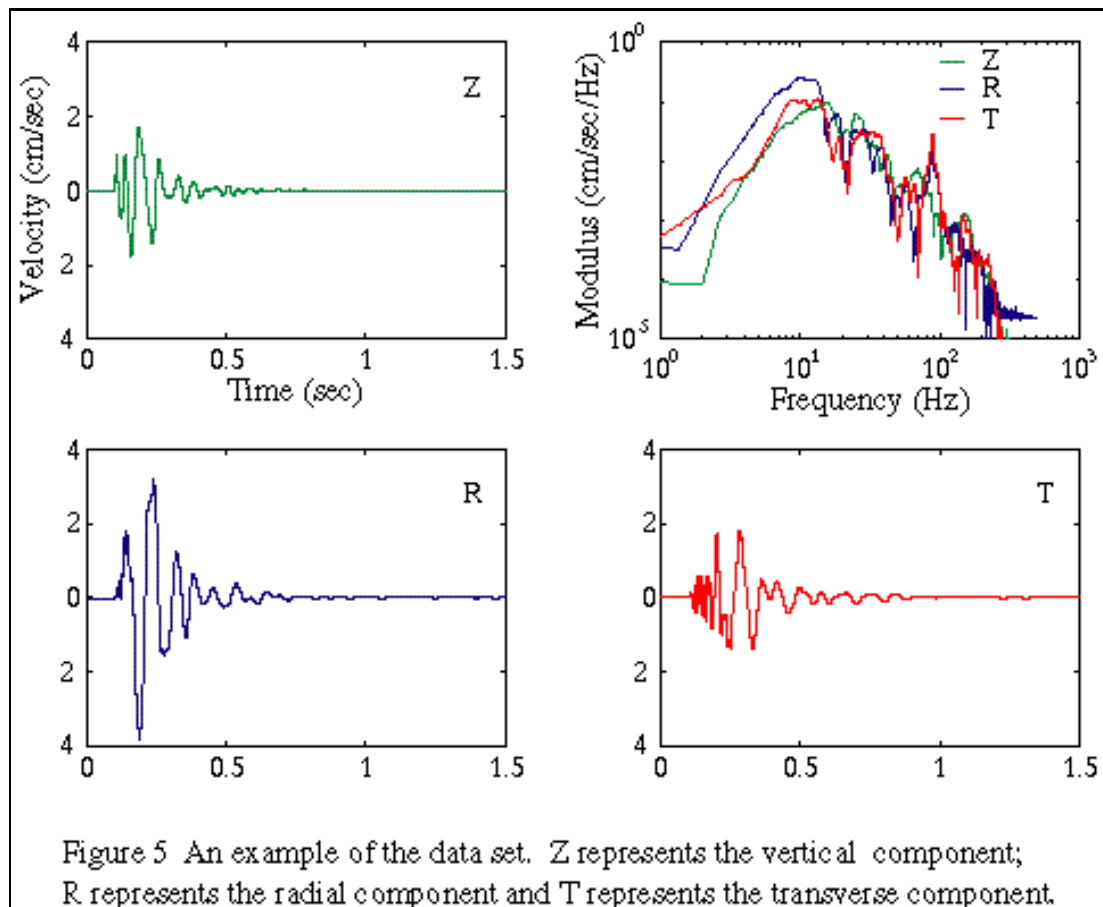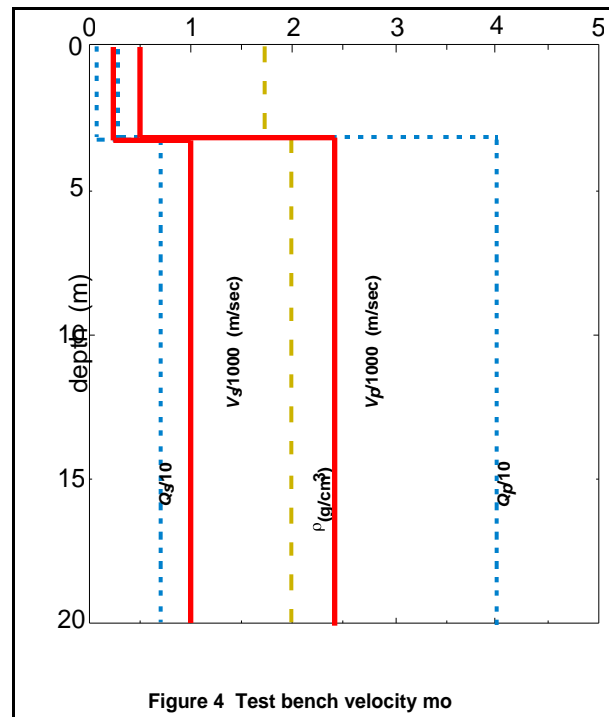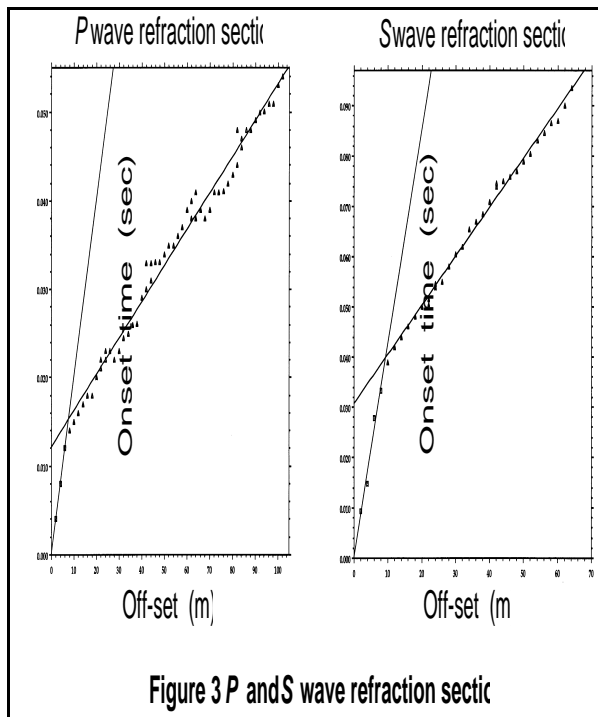

Figure 2 Vertical cross section of the source region config The medium consists of a low velocity layer overlying velocity half space. The source is located below the interfac two layers.

Figure 3 *P* and *S* wave refraction section

Figure 4 Test bench velocity mo

Figure 5 An example of the data set. Z represents the vertical component;
R represents the radial component and T represents the transverse component.
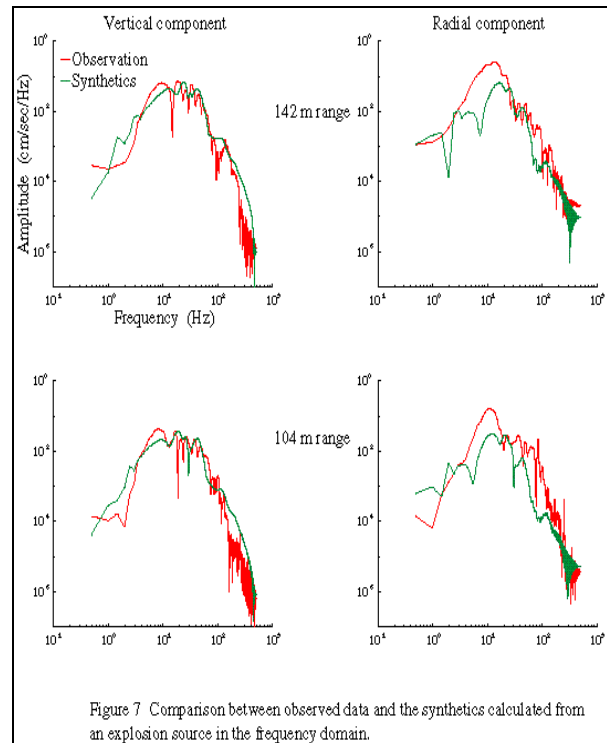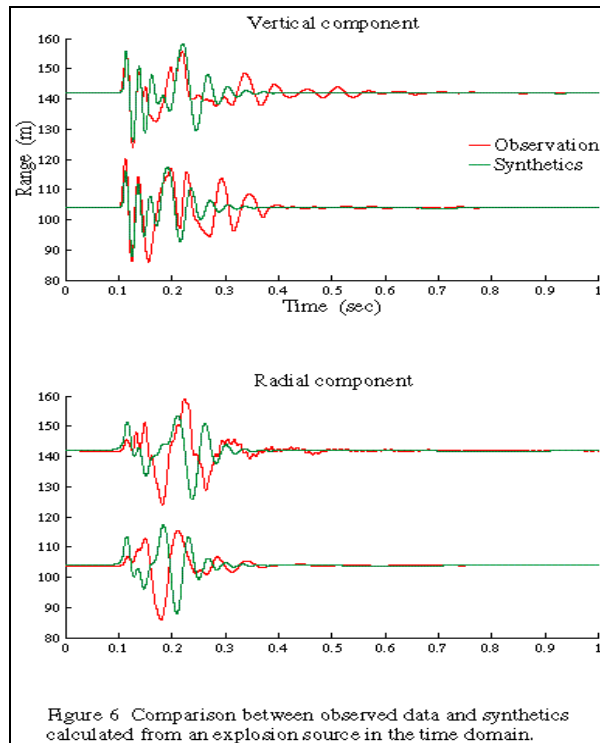
III. WAVEFORM MODELING

In order to obtain a reliable estimate of the propagation medium attenuation which is necessary for the inversion and to investigate the range of possible source processes, waveform data are modeled with explosion and spall moment tensor sources to constrain the source parameters and the medium quality factor Q.
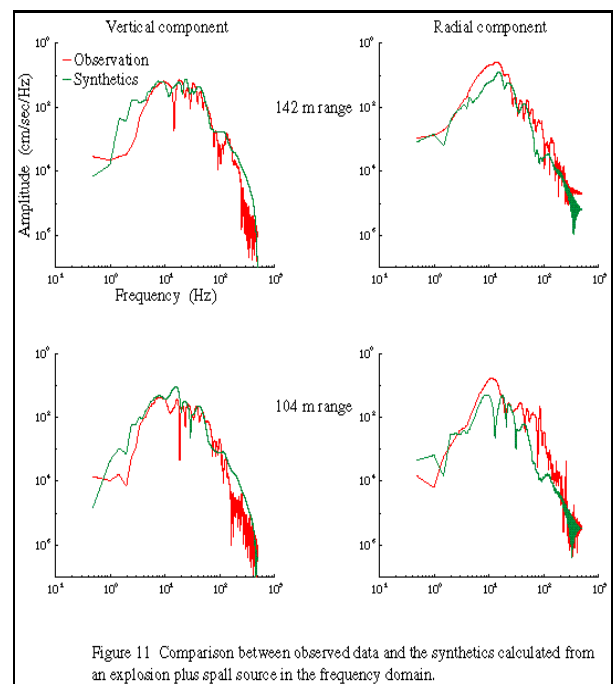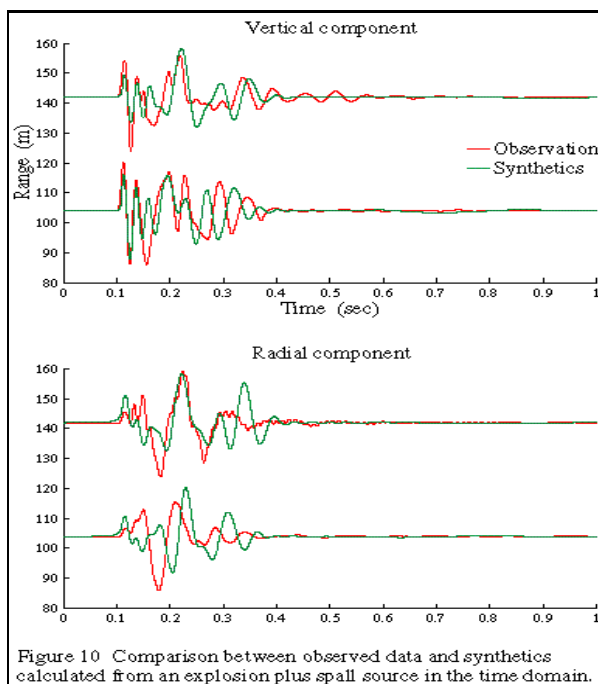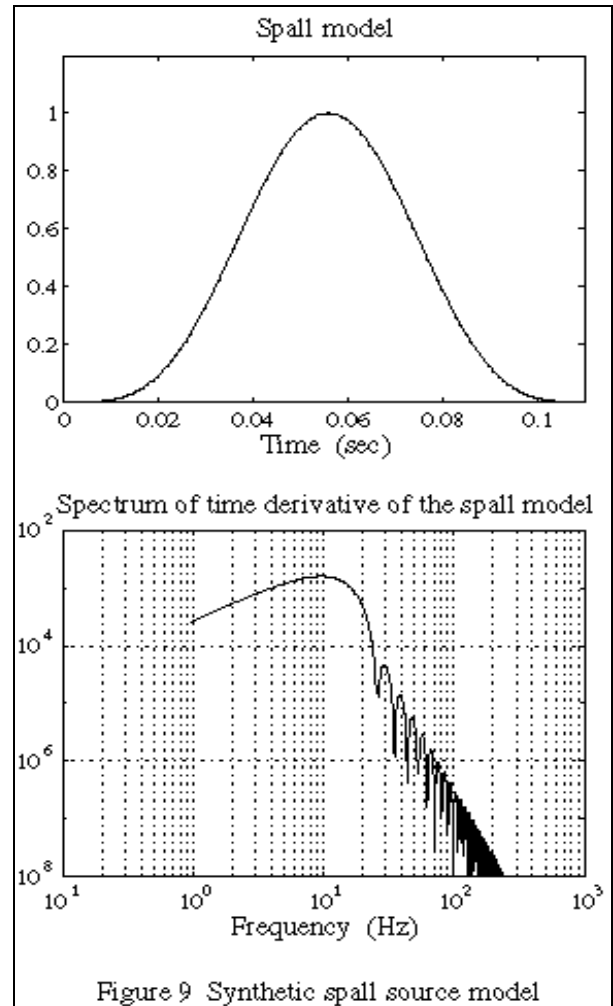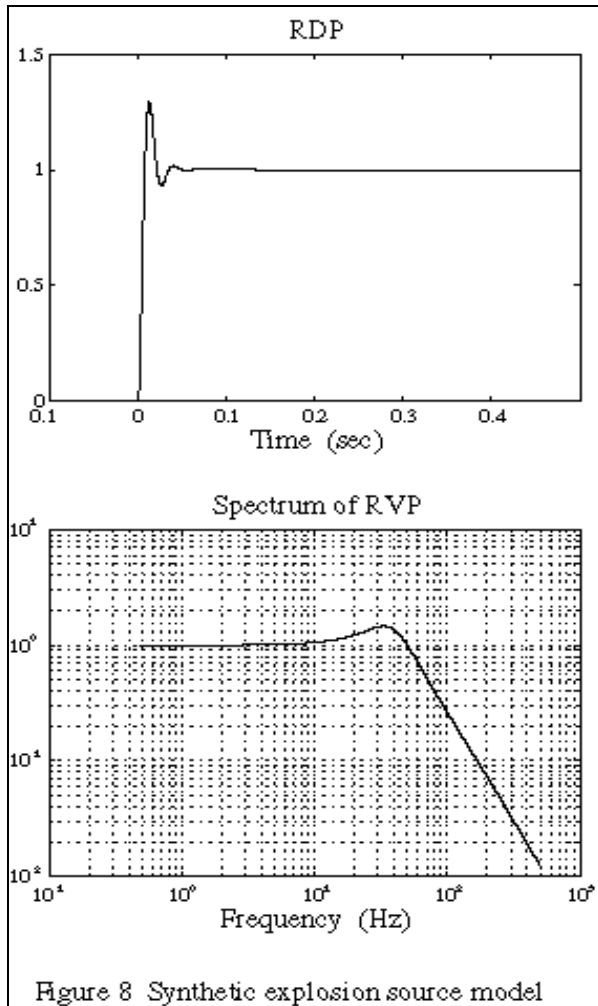
P wave contributions, mainly on the vertical component, are well modeled with an optimum combination of a Mueller-Murphy explosion source model and an attenuation model. The synthetics replicate the wave shape, frequency content and spatial decay rate of the observations (Figs. 6 and 7). The attenuation model is given in Fig. 4 while the explosion source model is presented in Fig. 8.

SV wave contributions, mainly on the radial component, are modeled with the addition of a spall moment tensor model. The time function of the model is expressed as

$$M_s(t) = \begin{cases} A\sin^{3.7}(\dfrac{\pi t}{T_0}) & (0 \quad t \quad T_0) \\ 0 & (t < 0; \ t > T_0) \end{cases}$$

and is plotted in Fig. 9. It is equivalent to a spall force model with equal rise and dwell times. Figs. 10 and 11 illustrate the improved fit of the explosion plus spall synthetics to the observed data especially on radial component.

Figure 6 Comparison between observed data and synthetics calculated from an explosion source in the time domain.

Figure 7 Comparison between observed data and the synthetics calculated from an explosion source in the frequency domain.

Figure 8 Synthetic explosion source model

Figure 9 Synthetic spall source model

Figure 10 Comparison between observed data and synthetics calculated from an explosion plus spall source in the time domain.

Figure 11 Comparison between observed data and the synthetics calculated from an explosion plus spall source in the frequency domain.

IV. MOMENT TENSOR INVERSION

Time dependent source moment tensors of the 8 mining explosion sources are estimated with the linear moment tensor inversion technique. The inversions are performed in the frequency domain and the moment rate spectra are estimated. Unique solutions are obtained for all the 8 sources. Fig. 12 shows the condition numbers of the inversions which reflect the quality of the estimates. An example of the results is given in Fig. 13.

The isotropic component of the source moment tensor spectrum which represents the volumetric component of the explosion is plotted in Fig. 14.

Frequency domain results are transformed back to the time domain and the source moment tensors are estimated. Moment tensor estimates for one of the shots are displayed in Fig. 15 to demonstrate some important features common to all the shots.
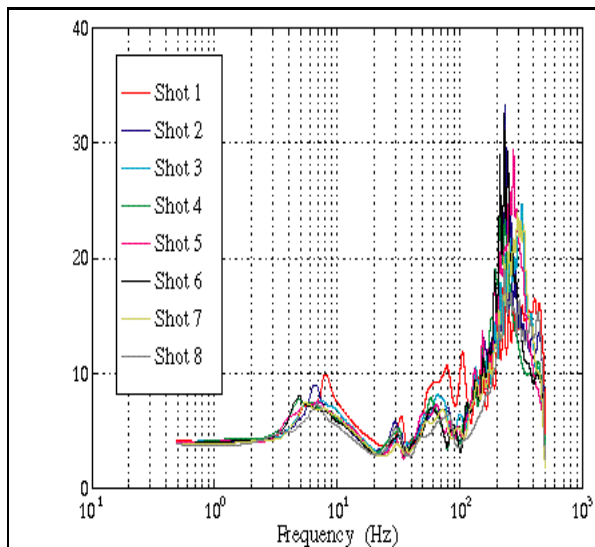

Figure 12 The condition numbers of the 8 inversions. The problems are well posed below 200 hertz which is signified by the small condition numbers.
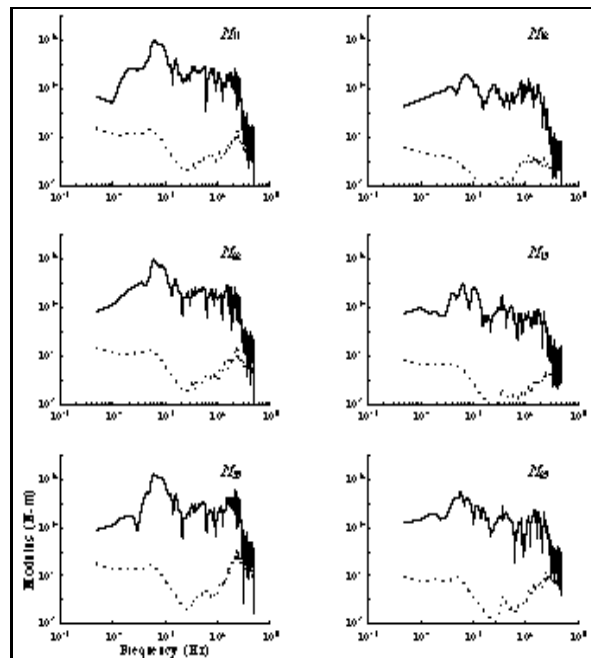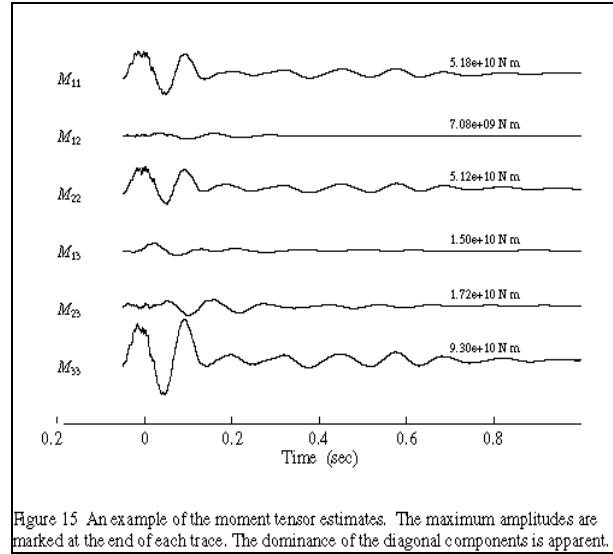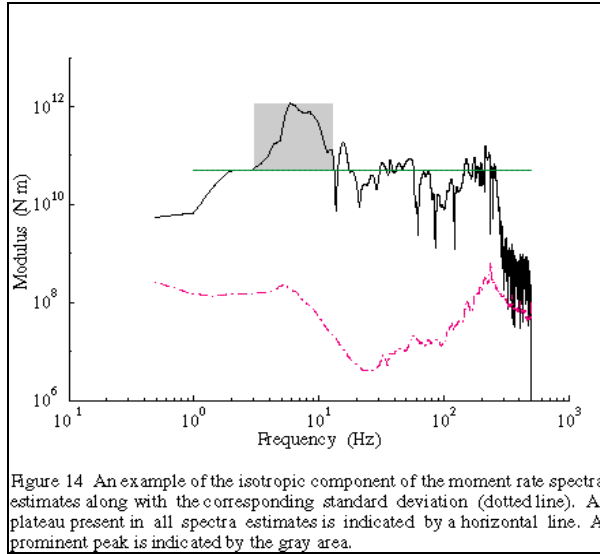

Figure 13 Moment rate estimates from one of the shots. The dotted lines are the standard deviations estimated with the real data variance.

Figure 14 An example of the isotropic component of the moment rate spectra estimates along with the corresponding standard deviation (dotted line). A plateau present in all spectra estimates is indicated by a horizontal line. A prominent peak is indicated by the gray area.

Figure 15 An example of the moment tensor estimates. The maximum amplitudes are marked at the end of each trace. The dominance of the diagonal components is apparent.
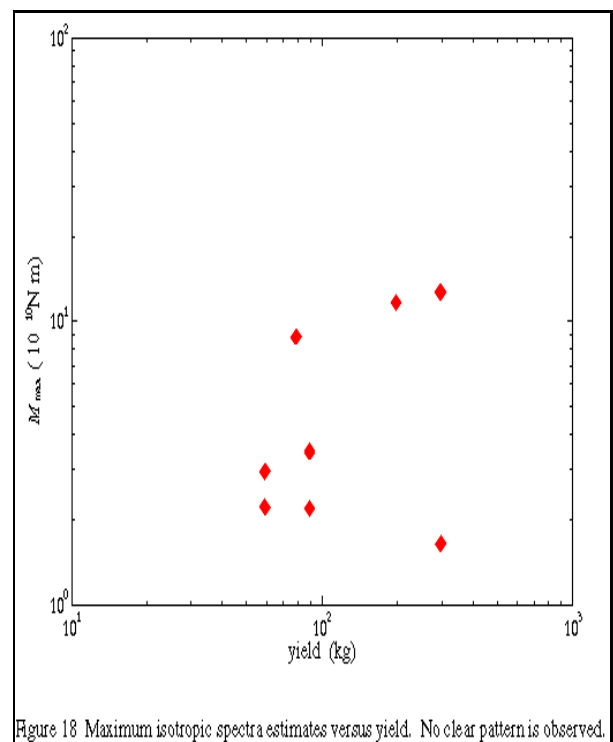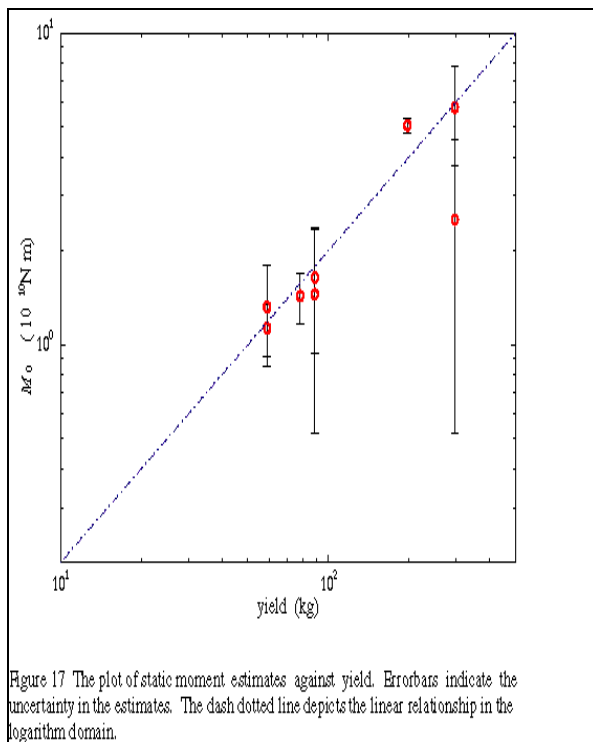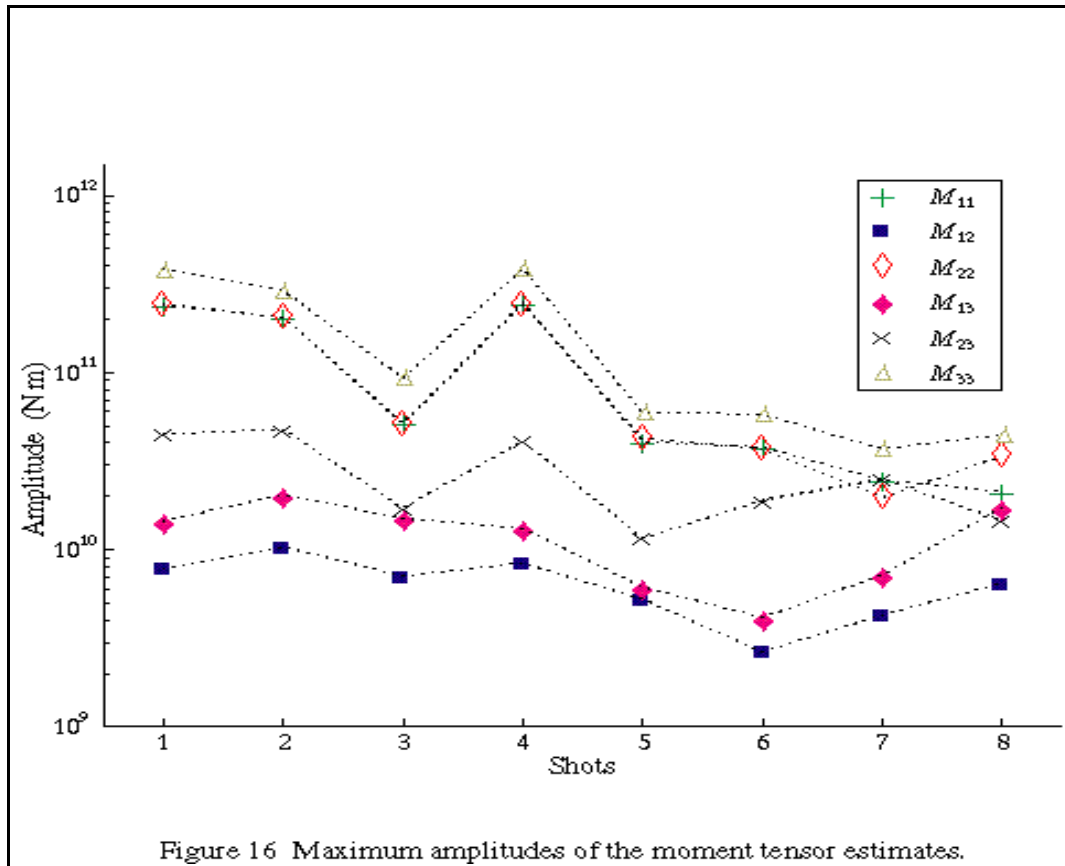
V. RESULTS & INTERPRETATIONS

Despite the particular source configuration (Fig. 2), all moment tensor estimates are dominated by the diagonal components, typical of an isotropic contained explosion source (Figs. 15 and 16). Among the diagonal components, the vertical dipole M_{33} is the largest, about 54% larger than the others. It may reflect the fact that the source region medium properties such as seismic velocity and density vary principally in the vertical direction.

The time histories of the diagonal component moment tensors show multi-peak patterns, suggesting complex source processes. The second peak in the diagonal component time histories partitions more energy onto the M_{33} component (Fig. 15). On average, the first peak of M_{33} component is 54% larger than the first peak of the other diagonal component while the second peak of M_{33} is 80% larger. This observation and the forward modeling result suggest that the second peak might be caused by spall. The frequency content and arrival time of the second peak are consistent with a spall model.

M_{23} is the largest off-diagonal component in the coordinate system with x_2 axis perpendicular to the vertical free face of the test bench and x_3 axis perpendicular to the earth's surface. It is twice as large as the other off-diagonal components, but still much smaller than the isotropic term (Fig 16). It may be related to the source region asymmetry caused by the presence of the free face and the free surface which affects the interaction between the burden and the rest of the medium. The small amount of M_{23} (16% - 44% of isotropic term) can account for most of the *SH* wave energy observed.

The isotropic moment rate spectra show a prominent peak around 9 hertz (the gray area in Fig. 14) and a plateau indicated by the horizontal line in Fig. 14. The plateau is believed to represent the static moment M_0 while the peak is consistent with the spall model. M_0 estimates based on this plateau range from 0.84×10^{10} N-m to 5.77×10^{10} N-m for the different explosions. The relationship between M_0 and yield is presented in Fig. 17 and is consistent with cube-root scaling. The peak in the isotropic spectrum does not show a clear pattern with yield (Fig. 18) indicating a more complex dependence of secondary source contributions, possibly affected by material properties.

Figure 16 Maximum amplitudes of the moment tensor estimates.

Figure 17 The plot of static moment estimates against yield. Errorbars indicate the uncertainty in the estimates. The dash dotted line depicts the linear relationship in the logarithm domain.

Figure 18 Maximum isotropic spectra estimates versus yield. No clear pattern is observed.

VI. CONCLUSIONS

Ground motion data from single mining explosion sources are modeled and the source moment tensors are estimated by inversion. The results indicate that despite some similarities, such as the dominance of the diagonal components, single mining explosion sources defer from contained explosions in many aspects.

Due to the closeness of the mining explosion sources to a vertical free face and the earth's free surface, the source process of the mining explosions seems to be more complex. Secondary source effects such as spall and the nonlinear interactions between the burden and the rest of the medium are important. A spall model with smooth rise time fits the observation well. Source region asymmetry due to the presence of the vertical free face and the free surface might result in the significant M_{23} component which accounts for most of the *SH* energy observed.

The effect of the cylindrical source geometry is not clearly observed in the source moment tensor estimates. The inadequate sampling of the source focal sphere by the data set might be one of the reasons. Future experiments might incorporate different source configurations and better receiver distributions to isolate different possible source processes and improve focal sphere coverage.